Numerical Study of Vortex Reconnection

Wm. T. Ashurst
Combustion Research Facility, Sandia National Laboratories, Livermore, California 94550

and

D. I. Meiron
Applied Mathematics, California Institute of Technology, Pasadena, California 91125
(Received 15 September 1986)

With a Biot-Savart model of vortex filaments to provide initial conditions, a finite-difference scheme for the incompressible Navier-Stokes equation is used in the region of closest approach of two vortex rings. In the Navier-Stokes solutions, we see that the low pressure which develops between the interacting vorticity regions causes the distortion of the initially circular vortex cross section and forces the rearrangement of vorticity on a convective time scale which is much faster than that estimated from viscous transport.

PACS numbers: 47.10.+g, 47.30.+s

There has been a great deal of interest in the dynamics of vortex tubes. One well-known method of approach is the representation of a tube as a space curve. The Biot-Savart law is then used to generate the velocity field which is used to convect the tube. In order to apply this method assumptions are made about the core structure of the tube. Usually it is assumed that the core remains circular and that there is no axial flow inside the core,[1] although more elaborate models have been considered. When these approximations are violated, experiments have shown that the core dynamics become significant. There have been several experiments reported in which two vortex rings traveling in the same direction become close enough to each other that in the region of closest approach there is a reconnection of the vortex tubes and the two rings become one contorted ring.[2-4] This reconnection process cannot be captured by vortex methods which use continuous filaments for a description of inviscid flow,[5] since without viscosity the vortex tube retains its identity for all time. In order for reconnection to occur dissipative effects must be considered.

In this work we study the dynamics of two closed vortex tubes which are approaching each other, using an Eulerian description of the incompressible Navier-Stokes equation. Our approach is numerical. We have implemented the fractional step method of Kim and Moin which defines the velocity components on a staggered grid.[6] Each component of velocity at a given location on the grid represents a cell-face mass flux. The pressure field is defined midway between cell faces.

Guided by the experiments of Schatzle and Coles,[2] we start the simulation using the inviscid Lagrangean dynamics[5] of the Biot-Savart law. The rings are initially planar in the y-z plane and move in the positive x direction; the initial ring radius is unity, the core radius σ is 0.1, and we set the circulation Γ to 4π. Time is scaled in units of Γ. The velocity at any point $\mathbf{x}$ is given by an integral over the filament arc length s of each ring,

$$\mathbf{U}(\mathbf{x}) = -\frac{\Gamma}{4\pi}\int \frac{\mathbf{r}\times\mathbf{t}}{(|\mathbf{r}|^2+\alpha\sigma^2)^{3/2}}\,ds,$$

where the distance vector $\mathbf{r}=\mathbf{x}-\mathbf{x}(s)$, the unit tangent vector $\mathbf{t}=d\mathbf{x}(s)/ds$, and the parameter α is 0.22 and represents a uniform vorticity distribution in the ring core. We have used two different models to determine the filament core diameter: (1) local core radius from local filament stretching to conserve vorticity volume, or (2) dynamical equations for the core area[7] which include axial flow within the vortex tube. The axial flow can be initiated by stretching which reduces the core radius and thus increases the swirling motion, thereby creating a local pressure minimum. The second model allows a step change in core size along the filament.

The ring centers start 2.5 units apart along the y axis and thus the initial closest separation distance is 0.5. Figures 1 and 2 display perspective views of one ring at time steps 150, 200, and 300. With an initial time step of 0.001 25, the vortex rings are starting to bend backwards in the region of closest approach after 150 time steps and significant core overlap exists after 50 more time steps. Our predictor-corrector scheme reduces the time step by a factor of 8 during the interval from 150 to 200 and additional node points are inserted to maintain the incremental arc length between nodes to be less than 0.75 of the local core radius. The overlap at step 200 is such that the maximum node velocity is 10 times larger than the initial value and the minimum separation distance between the two rings is $0.63\sigma_{\min}$ where $\sigma_{\min}$ is 0.045. Distortion of the filament only occurs over an arc which is less than 10% of the initial ring circumference. Continuation of the problem essentially leaves the region outside of the small arc interval frozen in time; i.e., the

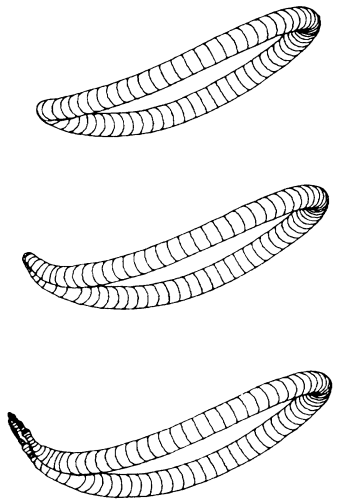

FIG. 1. Lagrangean calculation using vortex tubes with round cross section to simulate interacting vortex rings; no axial waves are included in this calculation. Perspective view of one vortex ring during its interaction with a mirror-image ring (not shown) on the left. The observer is above the path of the approaching rings. The initial radius is unity, and the ring separation in the top view is 0.14. Time increases from top to bottom; time steps 150, 200, and 300 are shown, the time values being 0.1875, 0.2091, and 0.2134. The arcs are located at the filament node points and reveal the insertion of new nodes with stretching.

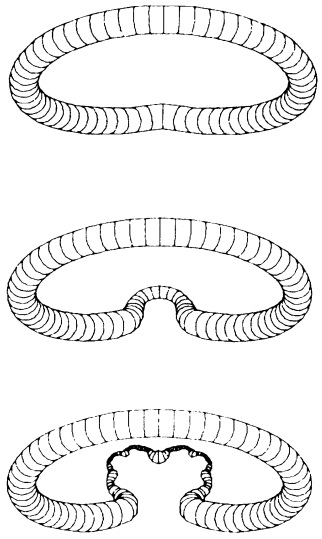

FIG. 2. Perspective side view of the ring shown in Fig. 1. Notice the decreasing core radius in the arc interval that has the closest approach with the second ring. The nodular shape may be forming a fractal object. Outside of the interaction region, the ring shape does not appear to change over the time interval shown.

arc length within this region grows with a resulting reduction in core size to conserve vorticity volume. At time step 300, there appears a seemingly self-similar growth pattern: We see nodules along the filament generated at points where the axial strain is zero.[8] It is this type of core dynamics which leads to a singularity in finite time as described by Siggia and co-workers.[9-11] However, with so much overlap and the constraint of circular cross section, there is some doubt if this shrinkage to zero core size is a physical result.

We have taken the Lagrangean inviscid results at time step 150 at which point the separation between the two rings is 0.14, which is 50% larger than the local core radius, and embedded this closest-approach region within a unit cube using 32^3 node points to describe the pressure field and the associated staggered grid for velocities in order to start a viscous Navier-Stokes simulation. The vortex filament tangent vectors and incremental arc lengths were used to generate the vector potential at appropriate locations so that the grid velocities are divergence free. We subtract off a uniform translation velocity in the x direction. From the two time levels of the velocity field in the moving reference frame, using a backward Euler time derivative, we obtain the pressure gradients from the finite-difference momentum equations. Thus, the velocities and pressures generated by the Biot-Savart law are used as initial conditions for the Navier-Stokes solution.

Using Schumann's estimate[12] for the combined convective-diffusive stable time step, we integrate the Navier-Stokes equation with a time step of 2×10^{-4} and with a Reynolds number (Γ/ν) of 10^3. We exploit the fact that the outer ring region does not appear to move during the evolution of the overlapping cores and keep the cube boundary conditions of velocity and normal pressure gradient constant. We find that the reconnection process is completed within a small enough time interval so that these surface constraints for this volume size are not a problem.

We exhibit the reconnection process given by the Navier-Stokes solution by showing the calculated grid vorticity in Fig. 3. The ring shown in Figs. 1 and 2 appears on the right side of Fig. 3. The time interval of the Navier-Stokes calculation corresponds to the interval between steps 150 and 250 in the Biot-Savart calculation. Instead of continual core collapse shown in Figs. 1 and 2, we obtain a topological change in the vorticity field with apparently little variation of core size along the newly connected filaments. A side view of Fig. 3 (not shown) indicates how the binormal effect moves apart the two newly connected filaments. In the experimental pictures of Schatzle and Coles, this motion continues until these regions are on opposite sides of the single vortex structure.

Low-pressure regions occur where the vorticity is largest and we use pressure to observe the nature of the vertical cross sections which pierce the two symmetry planes.

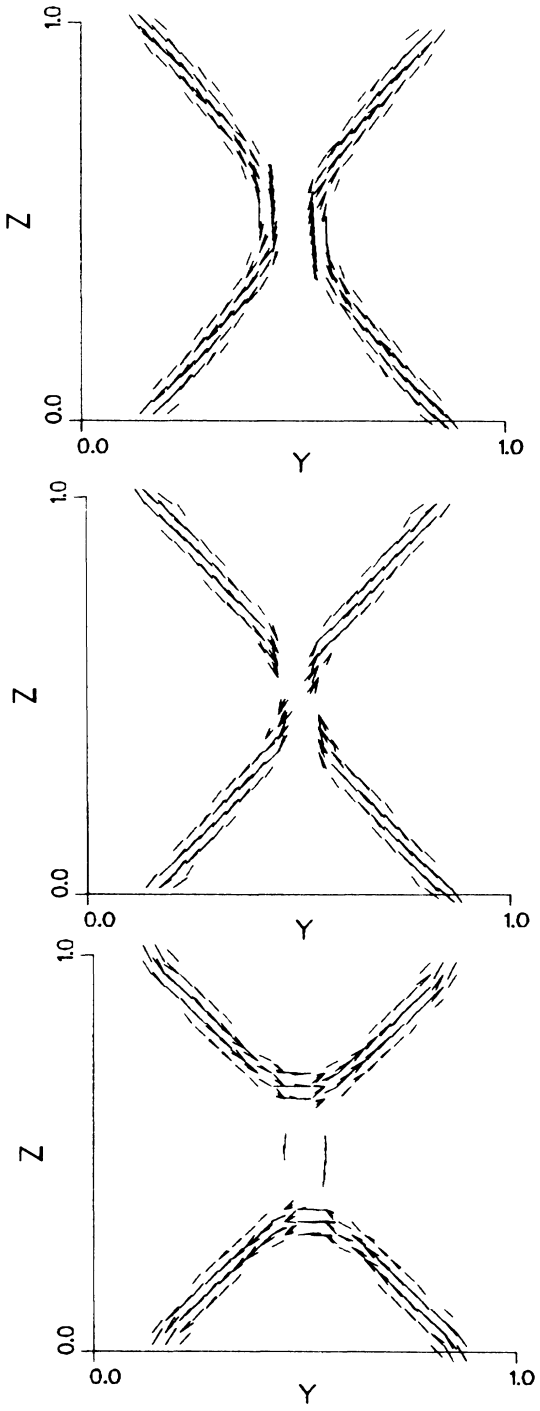

FIG. 3. Navier-Stokes calculation of the reconnection of interacting vortex tubes in the region of closest approach. The view is along the x axis. Grid locations which have vorticity magnitude greater than 0.6 of the maximum vorticity are shown by drawing a scaled vorticity vector (maximum length is $\frac{1}{16}$). The times shown, from top to bottom, are 0.004, 0.012, and 0.024 from the start of the Navier-Stokes calculation with a constant time step of 2×10^{-4}.

In the x-y plane, the z vorticity appears as a dipole with round cross sections when we first place the Lagrangean vorticity onto the Navier-Stokes mesh. The pressure minimum in the x-y plane gradually disappears as the z vorticity is rotated into the y direction and we see the formation of round pressure contours in the x-z symmetry plane. At the end of the Navier-Stokes calculation, the magnitude of y vorticity is 90% of the initial vorticity in the z direction.

We also performed simulations at Reynolds numbers of 10, 100, 1000, and 5000. The latter two do not appear to differ in contour plots of the solution, indicating that we may have reached the inherent numerical diffusion level in this scheme. With a Reynolds number of 100, the reconnection still occurs although the vorticity contours indicate more diffusion than in the higher Reynolds number case. The simulation run at a Reynolds number of 10 is completely different: Vorticity diffusion and cancellation is so large that vorticity disappears before it can be rotated to form reconnected tubes. Thus, we estimate that when the viscous time scale is a hundred or more times longer than the convective time scale then tube reconnection occurs.

We have varied the initial spatial configuration for the Navier-Stokes simulation and found that the duration of the reconnection does depend on the local shape of the interacting vortex tubes. Starting a Navier-Stokes calculation with two perfect circles which are in the same plane and separated in the plane by the distance found in the deformed-ring case (0.15), we find after an elapsed time of 0.048 that the reconnection is occurring but is not complete. The fixed surface conditions become a liability if the calculational period is much longer than this time interval. In the deformed case, the local tube curvature is such that the two sections are moving towards each other which is not the case in the two-perfect-ring calculation just described. The reconnection may be completely suppressed when the tubes are uniformly separated. Pumir and Kerr[13] have studied such a configuration by using one vortex tube which contains two signs of vorticity within its circular cross section. The tube center line is initially displaced from a straight line in a sinusodial fashion. They see vorticity forming into sheets in the tube cross-sectional plane without any obvious reconnection process. Thus, we conclude that reconnection dynamics will be sensitive to variations in the separation distance between sections of the tubes that are near the closest-approach region. A minimum reconnection time may occur if the tube configuration maximizes the velocity induced by tube sections that are far away from the reconnection region upon tube sections that become newly connected.

Returning to the description of our deformed-ring case, the simulation with Reynolds number of 1000, we infer a flow pattern by which the vortex tubes reconnect by examining the z vorticity in the x-y symmetry plane.

Near the z-y symmetry plane there is a line of node cells in which dV/dy has a very large negative value, and both dU/dx and dW/dz are positive and comparable in value. Thus, the z component of vorticity is reduced by a squeezing effect which rotates the vorticity into another direction. This squeezing motion is caused by static pressure differences which occurs when two vorticity regions of opposite sign approach each other, since they will induce a local maximum velocity between themselves, and hence a low pressure. The convective motion which results from this low pressure should scale by vorticity area and the amount of circulation contained within that area and not by a viscous time scale. So the time scale is σ^2/Γ rather than σ^2/ν and in our choice of parameters, these values are 10^{-3} and 1.

Siggia,[9] and more recently Siggia and Pumir,[10,11] have shown that if one assumes that the cores remain circular when two vortex tubes approach one another, then the growth of the core due to viscosity cannot be maintained against stretching along the filament axis. Thus, the core area shrinks to zero in a finite time resulting in a point singularity in the flow. The inclusion of axial waves does not suppress this singular behavior.[7] It is of course impossible to make conclusive statements about singular behavior from numerical simulation of the Navier-Stokes equations, but it appears that the pressure gradients and concomitant velocities arising from the close approach of two tubes of oppositely signed vorticity are sufficiently high to disrupt the tube and allow rearrangement of the vorticity on a convective time scale.

We speculate that reconnection may occur in a turbulent flow whenever two opposite-signed vorticity regions approach each other. From a preliminary calculation where the two rings had circulations in the ratio of 4:3, we see the stronger tube deform and undergo fission into two regions and then the start of the reconnection process between two opposite signed regions. In a calculation with 2:1 circulation ratio, we see the weaker tube becoming smeared around the stronger one; but away from the plane of interaction, the weaker-tube vorticity is enhanced by the axial stretching caused by the winding around the strong tube. A nonaxisymmetric spiral pattern of vorticity wrapped around a stretching vortex is the main ingredient in Lundgren's model which yields an energy spectrum with a $-\frac{5}{3}$ power range.[14] We note, however, that interactions with a circulation ratio of unity may be a common feature of turbulent flow. This case occurs, for example, whenever a single tube structure becomes bent into a U shape as is found in wall flows where horseshoe vortices are formed from transverse vorticity. Moin *et al.*[15] suggest that the legs of the horseshoe pinch off and form a vortex ring. Likewise, in the turbulent mixing layer, there is steamwise vorticity which may have the same evolution as in wall flows: Discrete vortex structures normal to the flow are drawn out in the flow direction and pinch off the trailing legs.

This work was supported by the U.S. Department of Energy, Office of Basic Energy Sciences, Division of Chemical Sciences. One of us (D.I.M.) was a visitor to the Combustion Research Facility at Sandia National Laboratories under the Summer Faculty Program. We wish to thank Dr. Nagi Mansour for helpful discussions on the Navier-Stokes scheme.

[1]D. W. Moore and P. G. Saffman, Philos. Trans. Roy. Soc. London, Ser. A **272**, 403 (1972).

[2]P. Schatzle and D. Coles, unpublished photographs and private communication.

[3]T. Fohl and J. S. Turner, Phys. Fluids **18**, 433 (1975).

[4]Y. Oshima and S. Asaka, J. Phys. Soc. Jpn. **42**, 708 (1977).

[5]A. Leonard, Ann. Rev. Fluid Mech. **17**, 523 (1985).

[6]J. Kim and P. Moin, J. Comput. Phys. **59**, 308 (1985).

[7]T. S. Lundgren and W. T. Ashurst, to be published.

[8]These results are obtained with the local core model; calculations with axial wave motion produce a helical twist with a more uniform core size in the stretching region.

[9]E. D. Siggia, Phys. Fluids **28**, 794 (1985).

[10]E. D. Siggia and A. Pumir, Phys. Rev. Lett. **55**, 1749 (1985).

[11]A. Pumir and E. D. Siggia, unpublished.

[12]U. Schumann, J. Comput. Phys. **18**, 465 (1975).

[13]A. Pumir and R. M. Kerr, following Letter [Phys. Rev. Lett. **58**, 1636 (1987).

[14]T. S. Lundgren, Phys. Fluids **25**, 2193 (1982).

[15]P. Moin, A. Leonard, and J. Kim, Phys. Fluids **29**, 955 (1986).